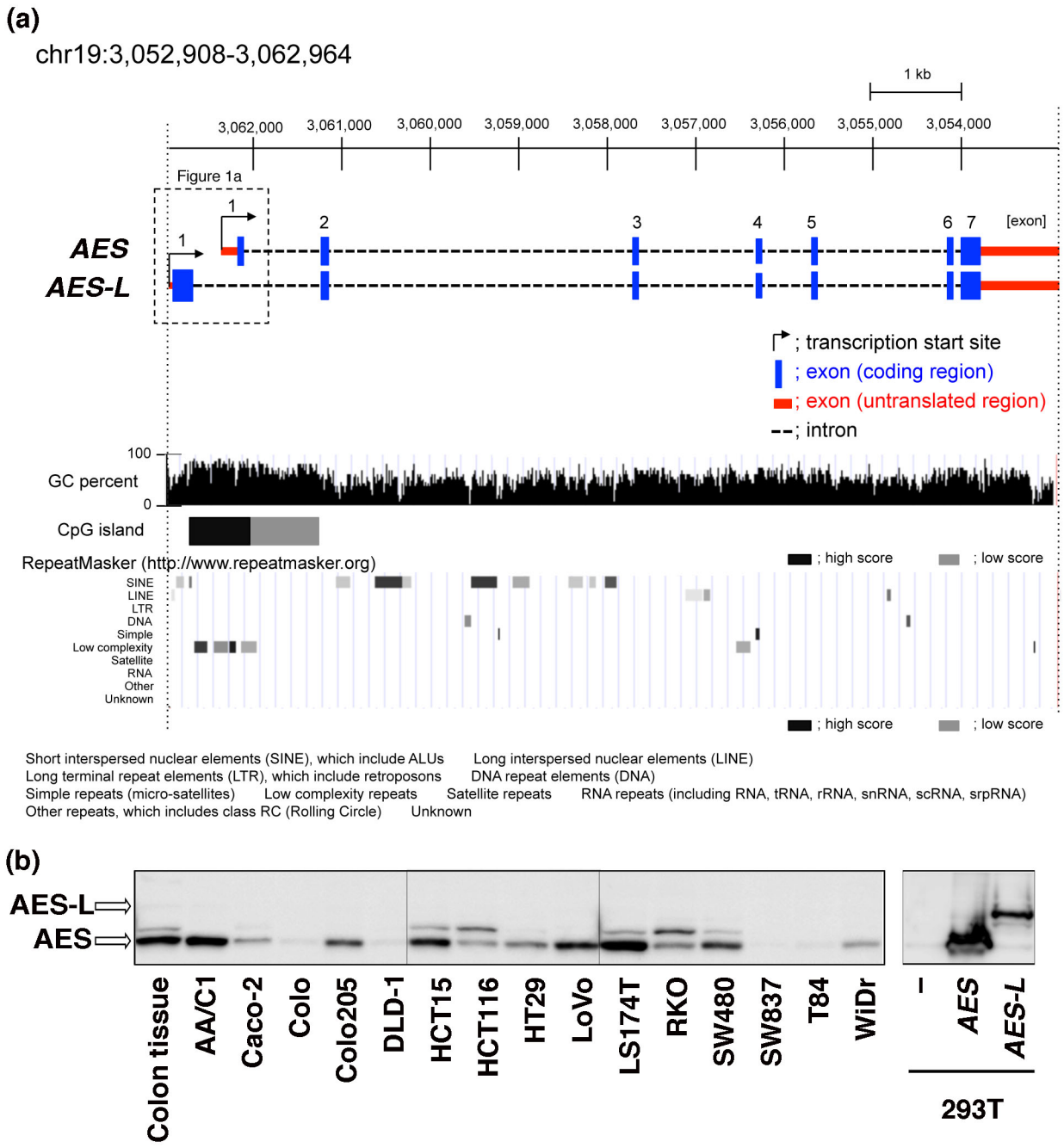

Fig. S1. Information on *AES-L* mRNA. (a) Schematic representation of *AES* exon-intron structure, GC percent, CpG island, and repeat markers in chromosome 19q13.3. A dotted rectangle indicates low magnification of Figure 1a. Schemata of CpG island and repeat markers were taken from UCSC genome browser (http://genome.ucsc.edu). (b) Western blot analysis of AES and AES-L in the normal mouse colon tissue and human CRC cell lines. A right panel shows the western blot analysis of AES and AES-L proteins in 293T cells in which the corresponding cDNAs were overexpressed.

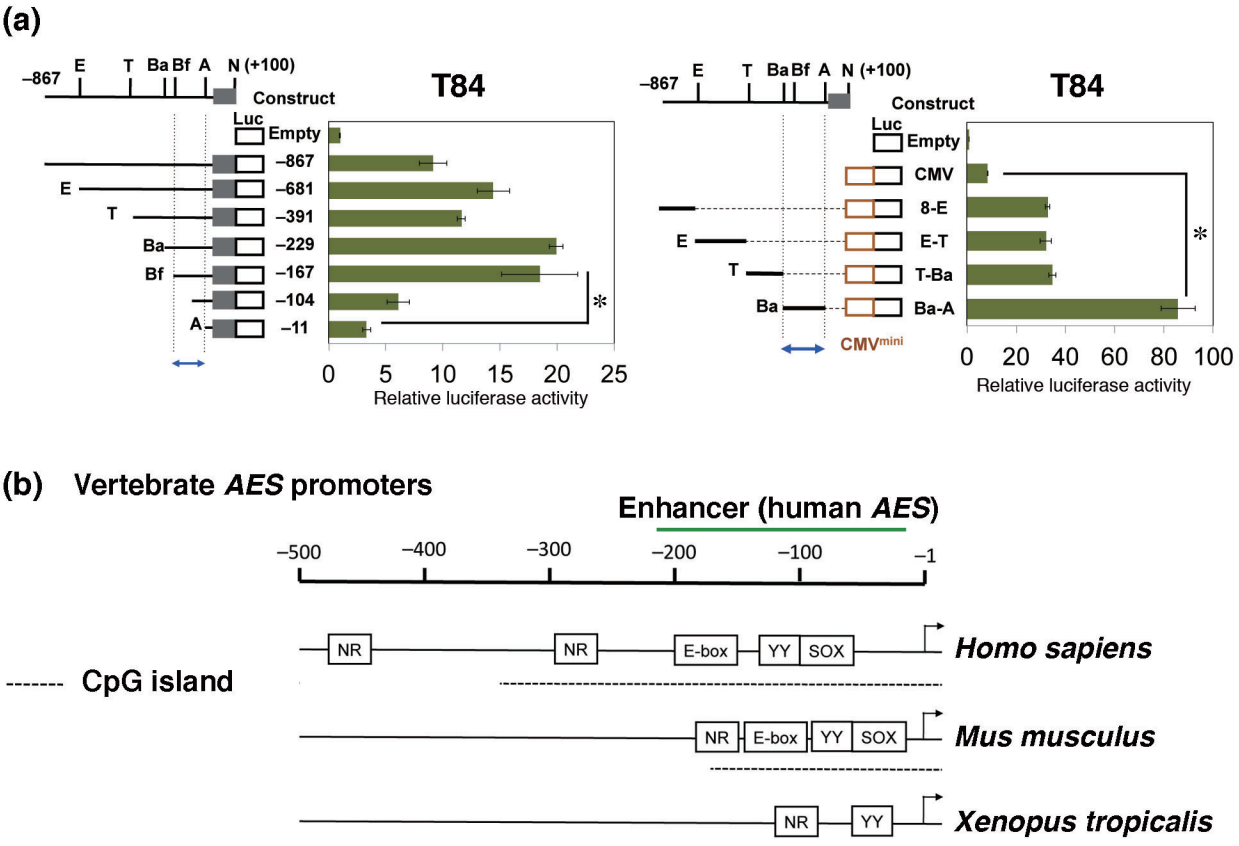

Fig. S2. *AES* promoter analysis. (a) Localization of regulatory elements in the *AES*-promoter region in T84 cells. The left panel shows luciferase expression constructs containing partial fragments with the endogenous *AES* promoter, whereas the right panel shows similar constructs with additional CMV-minimal promoter. The numbers indicate those of the nucleotides from the upstream-most transcription start site designated as +1. Filled green bars show relative luciferase activities calibrated to those of the promoter-less luciferase construct on top (Empty). Error bars show standard deviations of triplicated samples ($P < 0.01$).
(b) Evolutionarily conserved *cis*-elements in the *AES*-promoter of the human, mouse and frog genomes. Dotted lines indicate CpG islands. The numbers indicate the distance from the most upstream transcription start site (+1) of the human *AES* gene (Fig. 1c). Nuclear receptor (NR), E-box, YY, and SOX indicate the locations of binding motifs for the corresponding transcription factors.

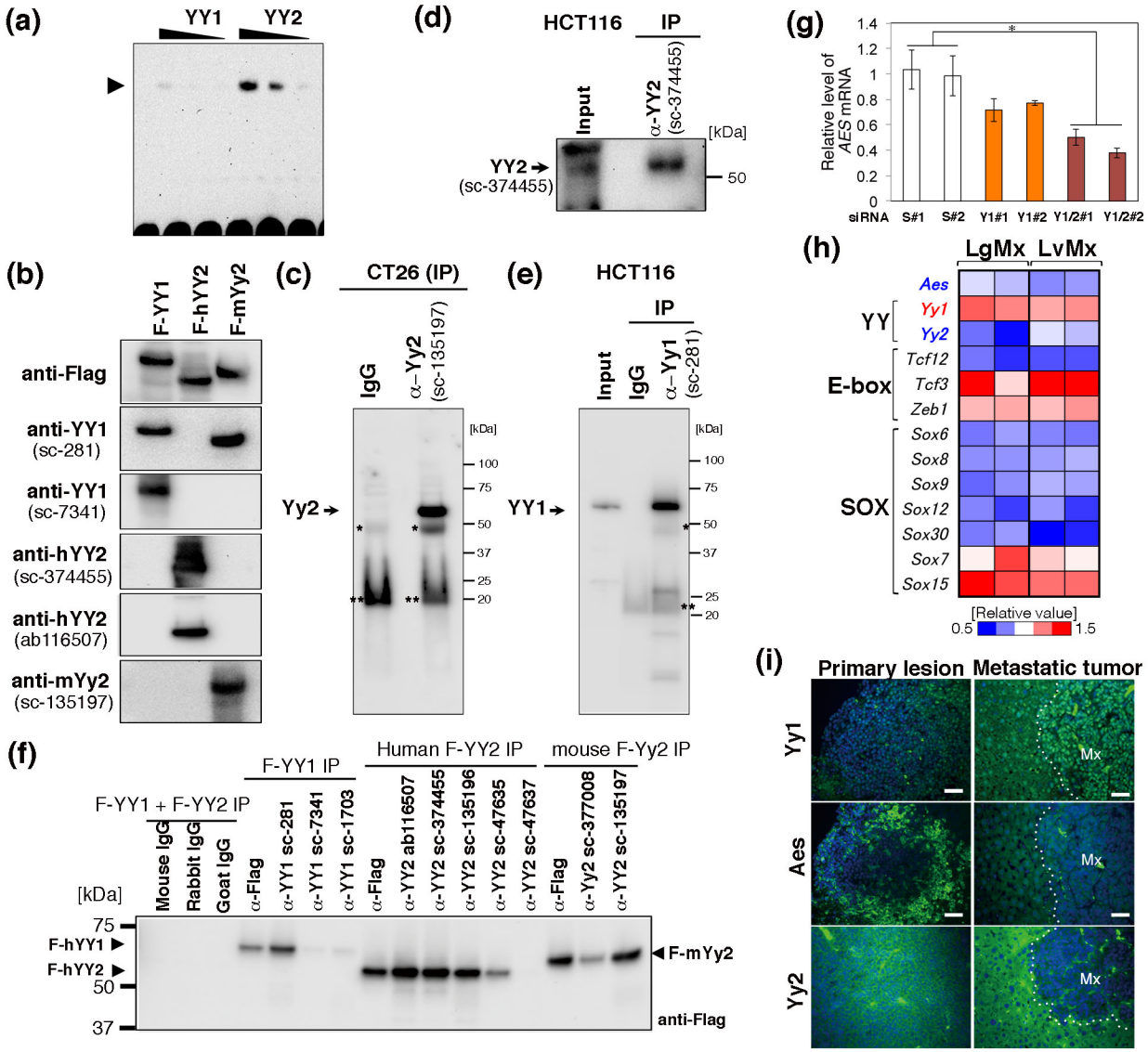

Fig. S3. Evaluation of anti-YY2 antibodies and expression of Yy2 in liver metastases of mouse CRC. (a) EMSA using the YY element of AES enhancer fragment and recombinant YY2 and YY1 proteins. Flag-tagged recombinant YY proteins were produced in bacteria as described previously.[8] Arrowhead indicates the position of the YY protein-DNA complexes. (b) Confirmation of antibody specificities for the recombinant Yy proteins. Anti-Flag antibody recognized all Flag-YY proteins (top). Note that anti-YY1 antibody (sc-281) reacted with both F-YY1 and mouse F-Yy2. The other YY antibodies recognized only the target YY proteins specifically. Antibody for mouse Yy2 successfully immunoprecipitated endogenous Yy2 protein in CT26 mouse colon cancer cells as shown in (c). (c,e) Immunoprecipitation followed by western-blot analysis of mouse Yy2 and human YY1 proteins using CT26- and HCT116-cell lysates, respectively. Asterisks indicate the positions for IgG heavy and light chains that cause non-specific signals. (d) Immunoprecipitation and western-blot analysis of human YY2 protein using HCT116-cell lysate.
(f) Immunoprecipitation with anti-YY antibodies. F-YY1, F-YY2 and F-Yy2 indicate recombinant Flag-tagged human YY1, human YY2 and mouse Yy2 proteins. Arrowheads indicate the molecular weights of F-YY1, F-YY2, and F-mYy2. (g) Summary of qRT-PCR determinations of the *AES* mRNA levels upon expression of siRNAs against YY1 and YY1/YY2 in HCT116 cells. "Y1/2#1", and "Y1/2#2" indicate independent siRNA constructs compared with scramble siRNAs (S#1 and S#2). *, P<0.01.
(h) Heat map of an RNA expression array analysis for transcription factors that recognize the evolutionarily conserved DNA elements in the *AES* enhancer region. (i) Immunofluorescence staining for Aes, Yy1 and Yy2 in the primary tumor and liver metastasis of CT26-transplantated mice. Mx, metastasis. Dotted lines indicate boundaries between metastasis and normal liver parenchyma. Scale bars, 40 μm.

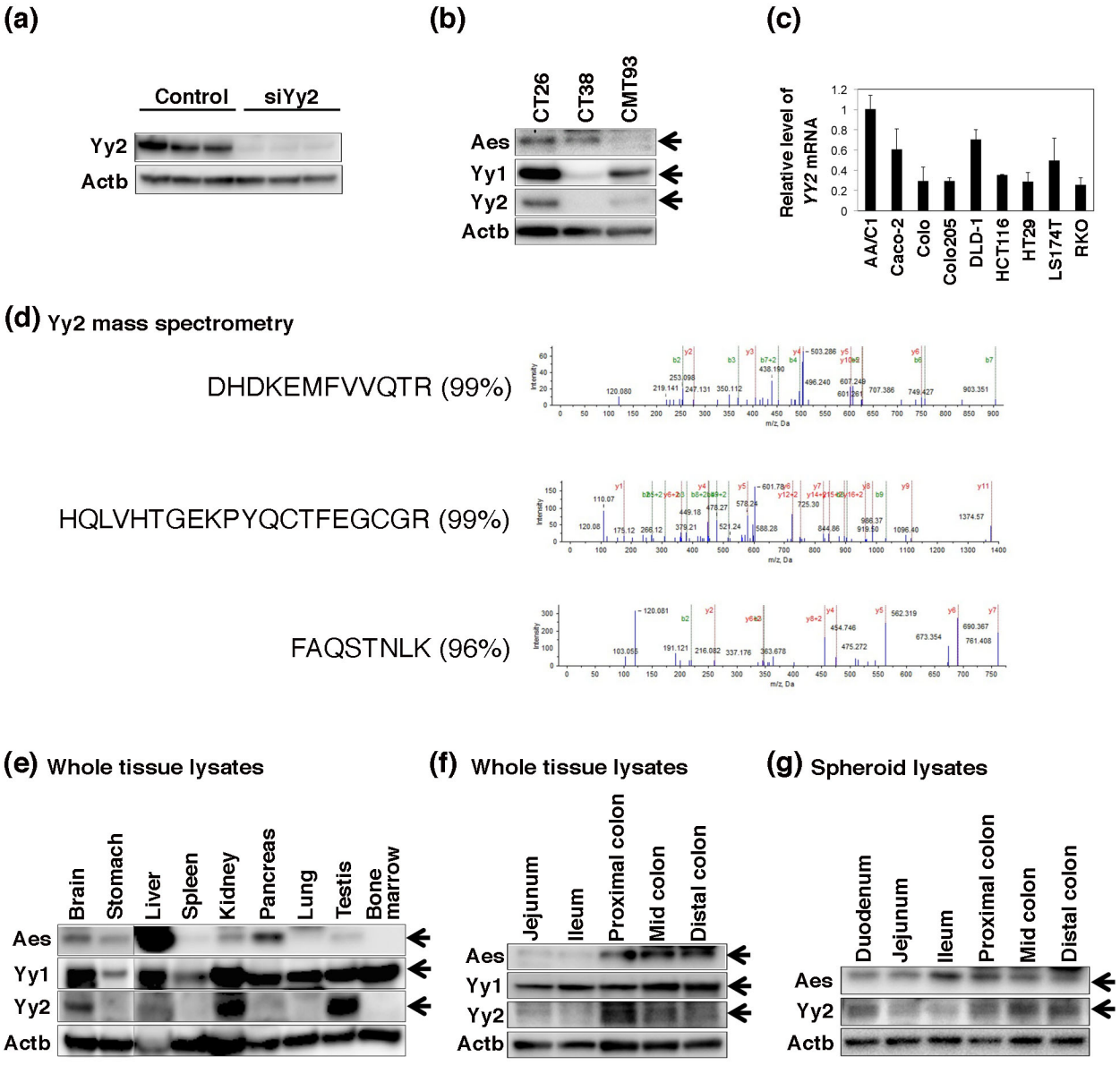

Fig. S4. Expression analysis of Yy2/YY2 in tissues and CRC cell lines. (a) Reduction in the Yy2 protein level in CT26 mouse CRC cells where expression of Yy2 protein was reduced by siRNA against the *Yy2* gene. Control and siYy2 indicate scramble siRNA and Yy2 siRNA, respectively. (b) Expression of Aes, Yy1, and Yy2 proteins in mouse CRC cell lines. (c) Expression levels of *YY2* mRNA in human CRC cell lines. (d) Mass-spectrometoric confirmation of mouse Yy2 protein. The Yy2 protein was prepared from testes by immunoprecipitation with an anti-Yy2 antibody (sc-135197). Mass-spectrometric analysis was performed as described in Supplementary Materials and Methods (Doc S1). (e–g) Expression of Aes, Yy1 and Yy2 proteins in mouse tissues (e) and (f), and epithelial-spheroids derived from various parts of the intestines (g).

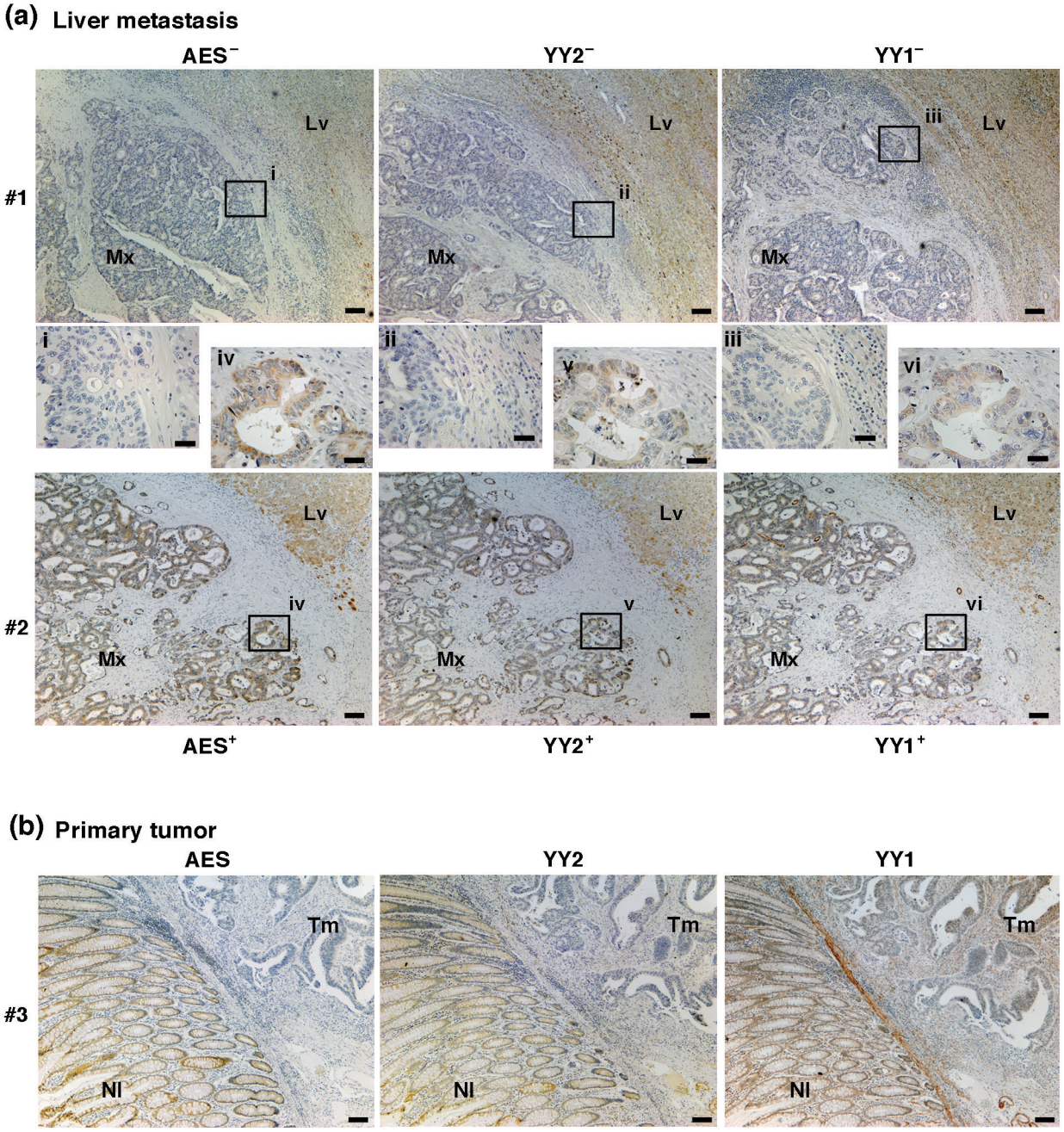

Fig. S5. Expression of AES and YY2 in human primary CRC and its loss in liver metastasis.
(a) Immunohistochemical staining for AES, YY1 and YY2 in the AES^- and $YY2^-$ (patient #1) and AES^+ and $YY2^+$ (patient #2) liver metastasis lesions of human CRC. Panels i-vi show higher magnification of the framed areas. Lv and Mx show liver and metastasis tissues, respectively.
(b) Immunohistochemical staining for AES, YY1 and YY2 in AES low and YY2 low primary tumors (patient #3). Nl and Tm indicate normal and tumor tissues, respectively. Scale bars, 20 and 200 μm for high and low magnifications, respectively.

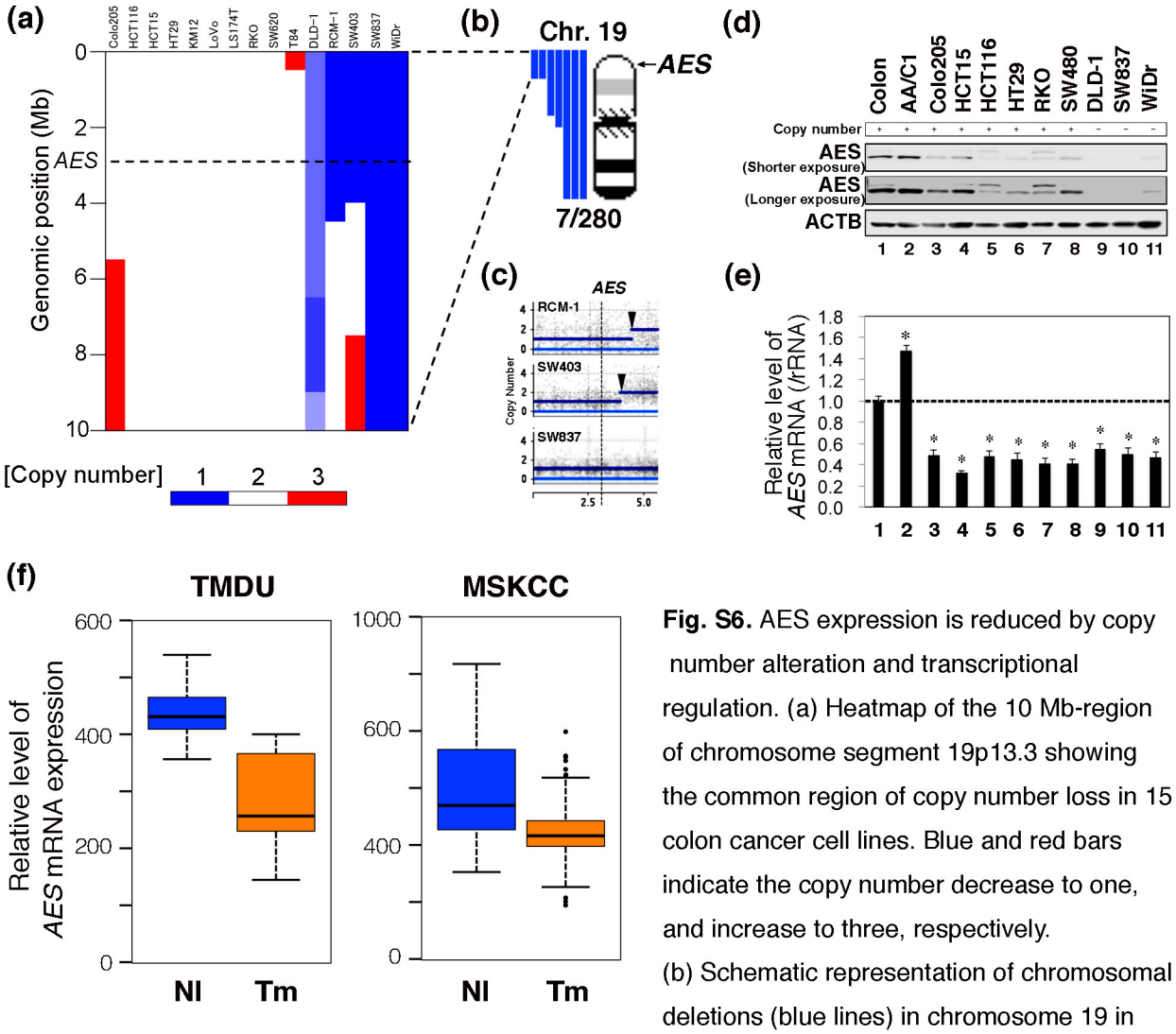

Fig. S6. AES expression is reduced by copy number alteration and transcriptional regulation. (a) Heatmap of the 10 Mb-region of chromosome segment 19p13.3 showing the common region of copy number loss in 15 colon cancer cell lines. Blue and red bars indicate the copy number decrease to one, and increase to three, respectively. (b) Schematic representation of chromosomal deletions (blue lines) in chromosome 19 in colon cancer obtained from NCBI SKY/M-FISH & CGH Database. Chr 19p13.3 is commonly deleted in the chr 19-loss patients. Arrow indicates the location of the *AES* genes. (c) Mapping of the partial diploidization in 19p13.3 found in colon cancer cell lines RCM-1, SW403, and SW837 using an Affymetrix SNP 6.0 array as compiled by Wellcome Trust Sanger Institute (http://www.sanger.ac.uk/cgi-bin/genetics/CGP/cghviewer/CghHome.cgi). Arrowheads indicate the break points. (d) Western blot analysis of AES protein expressed in 10 colon cancer cell lines, including three lines with single-copy loss of 19p13.3 (DLD-1, SW837, and WiDr). (e) A qRT-PCR quantification of *AES* mRNA in the same colon-cancer cell lines as in (d). The same positive controls were used in (d) and (e); a normal human colon tissue and colonic adenoma cell line AA/C1 (lanes 1 and 2, respectively). Asterisks indicate, $P < 0.01$. (f) Microarray analysis data for the *AES* mRNA levels extracted from the database of Tokyo Medical Dental University (TMDU) (17 normal-tissue and tumor sets, False Discovery Rate (FDR) = 8.0xE–6) and of Memorial Sloan-Kettering Cancer Center (MSKCC) (54 normal-tissues and 186 tumors, FDR = 2.3xE–8). Nl and Tm indicate normal colonic and tumor tissues, respectively.

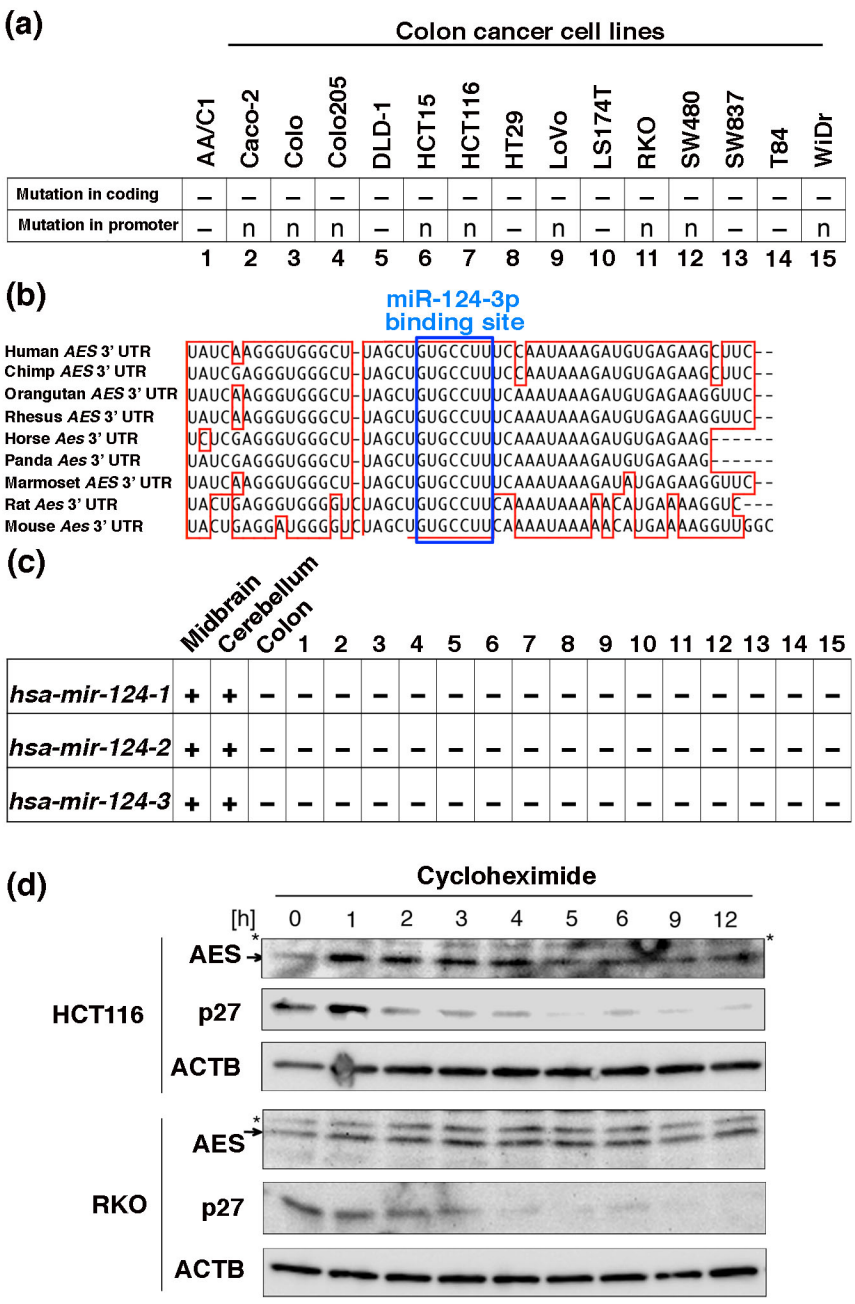

Fig. S7. Sequence analysis for coding and 3' UTR regions of *AES*, and protein-stability analysis. (a) Mutation analysis for the coding and promoter regions of *AES* in human colon cancer cell lines. Minus (–) indicates that no mutations were detected. "n" indicates "not determined". (b) The 3' UTR of *Aes* gene from six mammalian species aligned for the best match. A blue rectangle indicates a recognition sequence for microRNA mir124-3p. (c) Expression of mir124 members in human CRC cell lines. Minus (–) indicates no expression of the mir124 precursor transcripts at any detectable levels, whereas (+) shows substantial expression. In (a) and (c), colon adenoma cell line AA/C1 was also analyzed with negative results. (d) Stability of the endogenous AES protein in human colon cancer cell lines determined by western analysis. The Aes protein bands at the indicated hours after cycloheximide (CHX) treatment in HCT116 (upper) and RKO (lower) cell lines. As a positive control for a cell cycle-dependent degradation after CHX treatment, p27 was used. Asterisks indicate the band of a non-specific protein detected by the antibody. ACTB shows the band for β-actin used as the loading control.

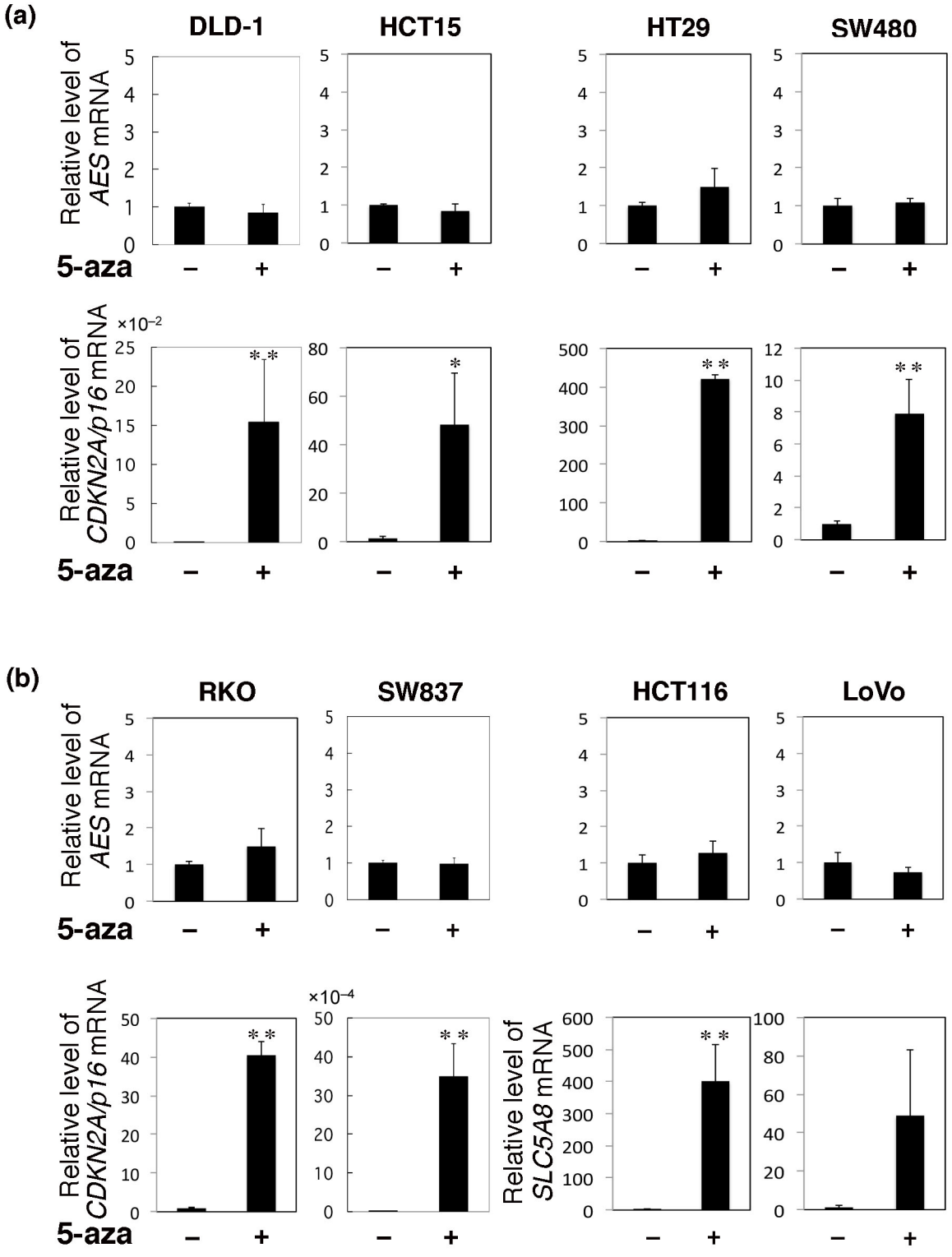

Fig. S8. De-methylation analysis of *AES* promoter. (a–b) (Top) A qRT-PCR quantification of *AES* mRNA in eight colon cancer cell lines treated with a DNA de-methylating reagent 5-aza-deoxycytidine (5-aza) for 96 hours (+), compared with the no-drug controls (–). (Bottom) Data from similar experiments showing strong induction of *p16* (*CDKN2A*) and *SLC5A8* mRNA as positive controls.

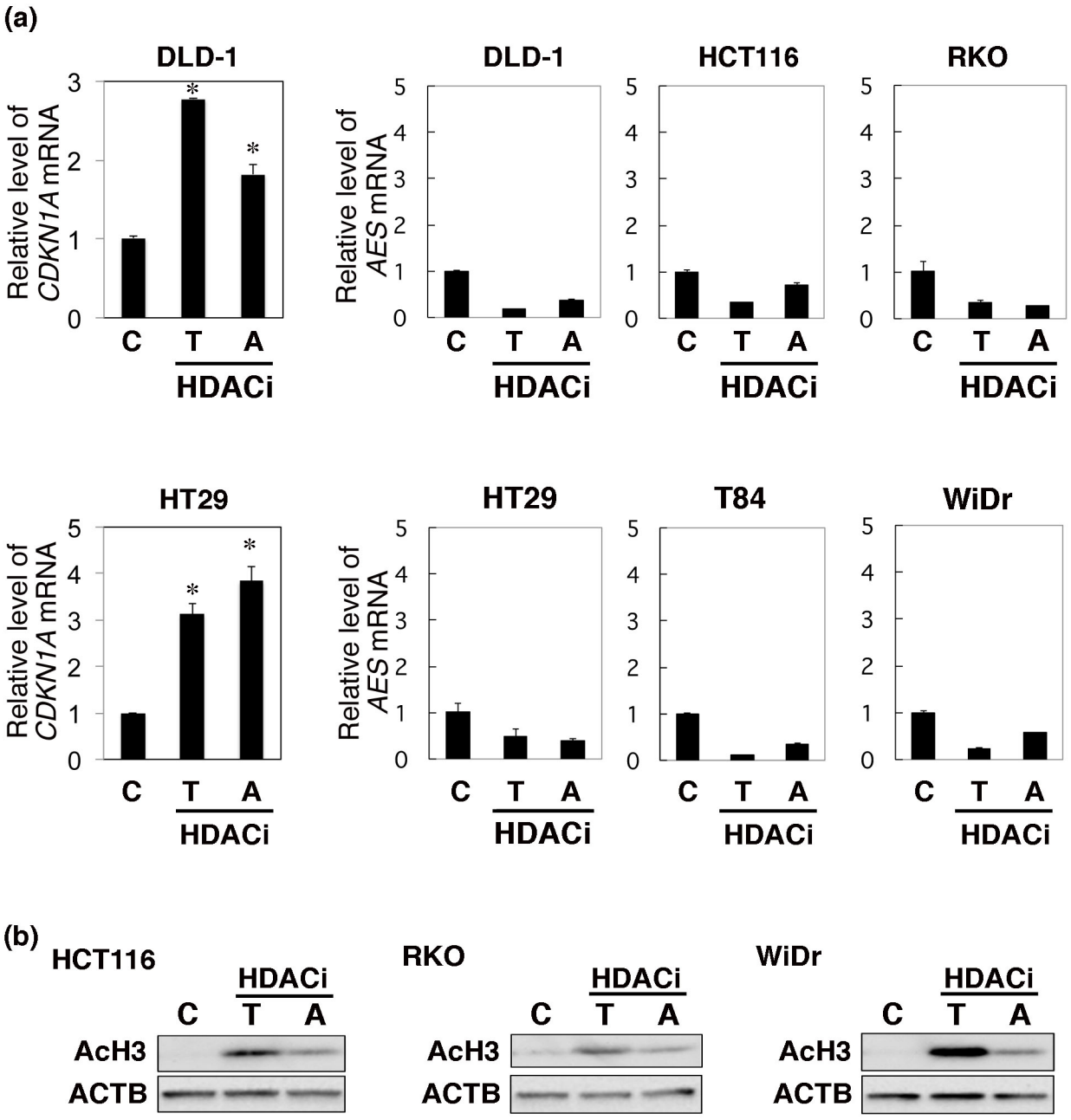

Fig. S9. Histone-acetylation analysis of *AES* promoter. (a) Reduction of endogenous *AES* levels by HDAC inhibitors (HDACi); T and A for trichostatin A (TSA) and apicidin, respectively. Left-most graphs indicate the levels of *CDKN1A* mRNA in HDACi-treated DLD-1 (top) and HT29 (bottom) cells, relative to those in non-treated controls (C) at 24 h post-transfection. Right side graphs indicate expression of *AES* mRNA in HDACi treated colon cancer cells. Error bars show standard deviations of triplicate samples. Asterisks indicate significant differences from the controls ($P < 0.01$). (b) Western blot analysis of histone H3 acetylation (AcH3) in HCT116, RKO and WiDr cells. ACTB was used as a loading control.

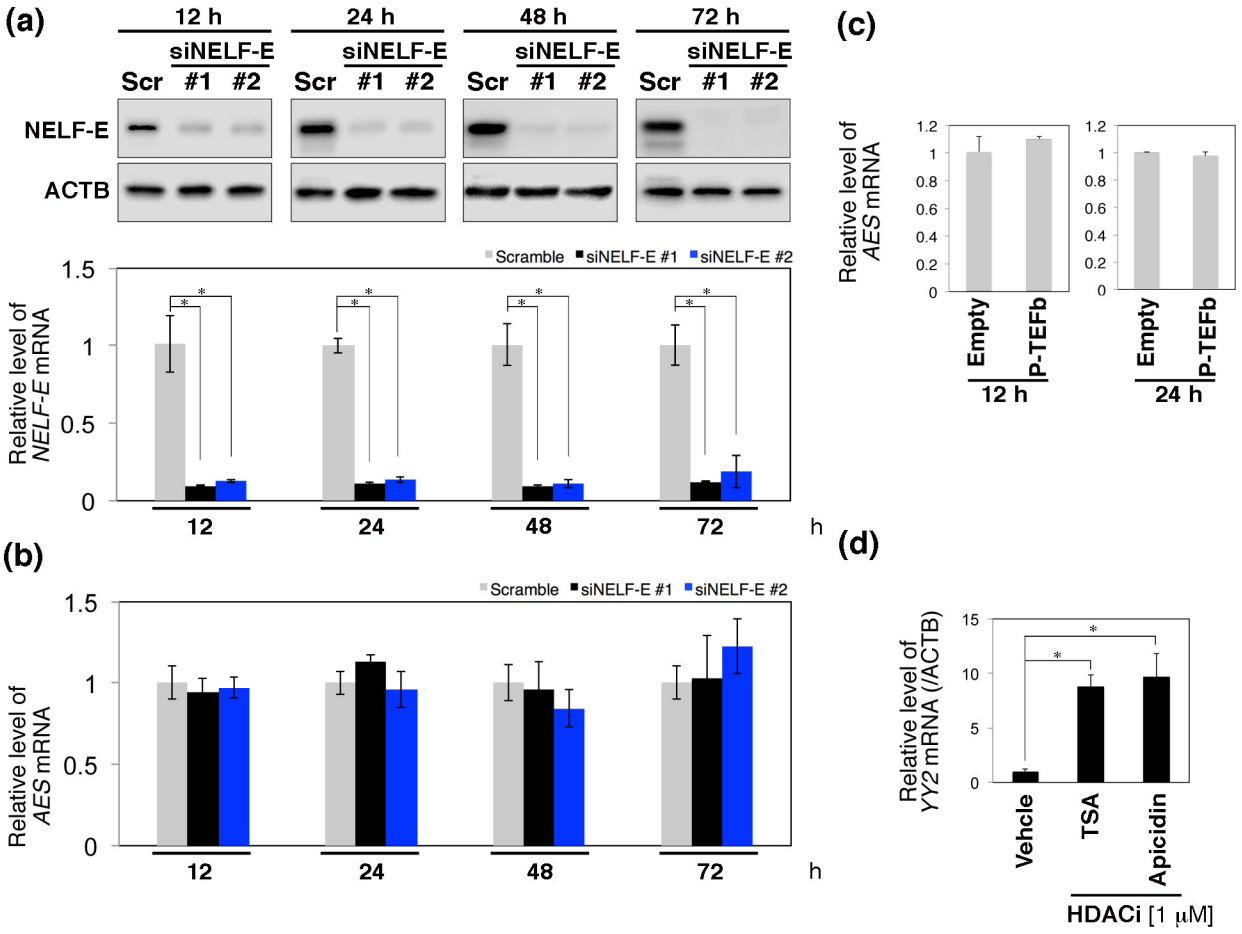

Fig. S10. Testing for promoter-proximal transcriptional pausing in the *AES* promoter, and induction of YY2 transcription by HDACi. (a–c) Effects on the *AES* promoter of canceling promoter-proximal transcriptional pausing by NELF-E knockdown and P-TEFb overexpression. (a) (Top) A western blot analysis of NELF-E protein at the indicated hours after the *NELF-E*-siRNA introduction of HCT116 cells. "Scr" indicates scramble siRNA. (bottom) A qRT-PCR quantification of *NELF-E* mRNA at the indicated hours after the *NELF-E*-siRNA introduction of HCT116 cells. (b) A qRT-PCR quantification of *AES* mRNA at the indicated hours after the *NELF-E*-siRNA introduction of HCT116 cells. (c) A qRT-PCR quantification of *AES* mRNA levels at the indicated hours after the induction of P-TEFb overexpression in HCT116 cells. (d) Induction of *YY2* mRNA expression by HDACi TSA and Apicidin in RKO cells. Error bars show standard deviations of triplicate samples. Asterisks indicate significant differences from the controls ($P < 0.01$).